Proceedings of IMECE'04
2004 ASME International Mechanical Engineering Congress
Anaheim, CA, November 13-19, 2004

IMECE2004-62470

DYNAMIC BEHAVIOR AND SIMULATION OF NANOPARTICLE SLIDING DURING NANOPROBE-BASED POSITIONING

Afshin Tafazzoli
Department of Mechanical Engineering
Nanorobotics Laboratory,
Carnegie Mellon University,
Pittsburgh, PA 15213-3890, U.S.A.

Metin Sitti
Department of Mechanical Engineering and the
Robotics Institute, Nanorobotics Laboratory,
Carnegie Mellon University,
Pittsburgh, PA 15213-3890, U.S.A.

ABSTRACT

In this paper, the behavior of nanoparticles, manipulated by an atomic force microscope nanoprobe, is investigated. Manipulation by pushing, pulling or picking nanoparticles can result in rolling, sliding, sticking, or rotation behavior. The dynamic simulation of the nanoparticle manipulation, using atomic force microscope (AFM), is performed. According to the dynamics of the system, the AFM pushing force increases to the critical value required for nanoparticle motion. Nanoparticle positioning is designed based on when the nanoparticle is stopped by the AFM in order to move on the substrate. Simulation results for gold particles on a silicon substrate showed that sliding on the substrate is dominant in nanoscales.

INTRODUCTION

Nanoparticle manipulation using the AFM has been of widespread interest for the last few years [16], [20], [25]. Using AFM as a nanomanipulation tool enables us to locate nanoparticles in a desired position for micro/nano assembly [24], [29]. Controlled pushing of nanoparticles is also used for nanotribological characterization purposes [26], [28].

Dynamic modeling of nanoparticles is being developed ([10], [21], [22]), and is a major tool for understanding the manipulation procedure. The physics of nanoscale dynamics and governing equations are different from the macroscale's, as adhesion forces and contact deformations should be considered [7].

In this work, nanoscale forces are accounted to build a real time nanomanipulation simulation. Its novelty is that the nanoparticle can be traced at every moment. At the same time, all the dynamics and deformations can be achieved from numerical simulation that is accompanied by a real time visual simulation of the manipulated nanoparticle. In contrast to macroscale, it is proved that nanoparticles start to slide first on substrates rather than rolling.

As the outline of the paper, initially, nanoparticle manipulation is defined, and the AFM probe, AFM tip, nanoparticle, and substrate motion are modeled separately. Later, all the models are combined, and the dynamic analysis of the system is conducted. Finally, simulation results are demonstrated and discussed.

PROBLEM DEFINITION

The AFM contacts with a nano-particle and stops the particle from moving with the substrate (figure 1). After non-contact-mode scanning of the substrate and the targeted particles, the AFM approaches and makes contact with the target particle. Contact angle φ is designed to be constant and greater than zero for pushing purposes. To be certain of the desired contact, a small normal preload, F_{z0} is exerted by providing normal deflection offset, z_{P0} on the AFM probe. In stage I (demonstrated by the dashed line), both the substrate and particle are stationary. Following stage I, the substrate starts to move with constant velocity and the particle sticks and moves with the substrate, indicating the beginning of stage II. In stage II, the AFM deflections due to particle motion, can be sensed and recorded using optical methods [4], [6], [17], [27]. Lateral motion of the particle assists the increase of the AFM lateral and pushing forces, F_T.

At the end of stage II, pushing force reaches the critical force required to separate particle from substrate. Therefore, the particle is stopped from moving with the substrate and, depending on the dynamic mode diagram of the particle, the suggested behavior will follow.

All possible behaviors are analyzed in [31] by the authors. The designed parameters in this paper avoid undesirable slipping on the tip and rotation; slipping on the substrate,

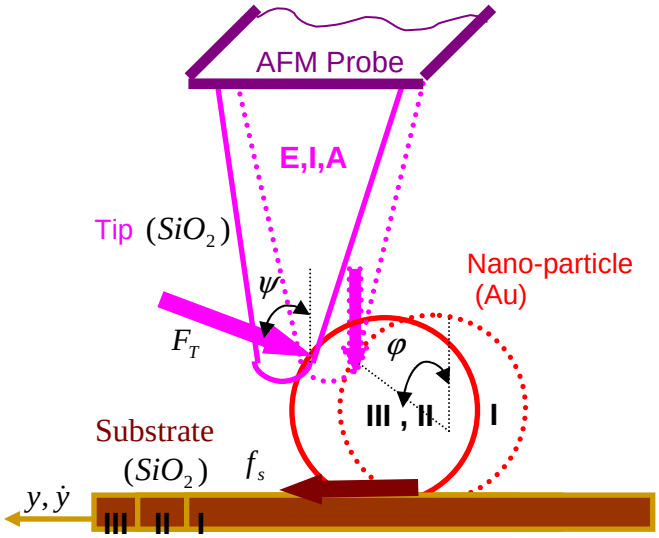

Figure 1. AFM stops nano-particle from moving with the substrate after stage II.

however, is expected. Therefore there is no rolling expected, and sliding behavior is considered.

After stage II, the substrate moves separately to stage III, while the nanoparticle slides on the substrate. This can be interpreted as the particle moving with negative, but similar velocity in the opposite direction relative to the substrate. This method is used for high-precision positioning of nanoparticles [19], [32].

METHODS

A. *Atomic Force Microscope (AFM) Model*

The AFM, which is commonly used as a 3D topography imaging device, is used as a manipulation tool for nanoparticle positioning; it consists of a conical tip connected to a cantilever probe at the end (figure 2).

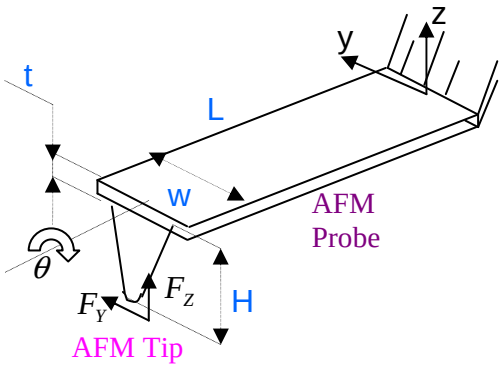

Figure 2. AFM probe & nanoforces at the probe tip.

In the sticking phase, the AFM tip traces the moving particle which leads to probe motion. The AFM tip contacts with the nanoparticle and moves with the same velocity and direction, resulting in twisting and bending of the cantilever probe.

In figure 3, the AFM probe is modeled as one torsional and two linear springs [1], [23]. Damping forces are not considered in this model since manipulation takes place at low speed and constant velocity. Linear springs account for normal and lateral motion, and lateral twisting is recorded by the torsional spring. Stiffness coefficients of the springs are a function of AFM mechanical properties (E,G), and geometry (L,w,t,H) (eqs. 1-3).

$$K_z = \frac{Ewt^3}{4L^3} \tag{1}$$

$$K_y = \frac{Ew^3t}{4L^3} \tag{2}$$

$$K_\theta = K_y^{\,torsion} H^2 = \frac{Gwt^3}{3L} \tag{3}$$

where L is the length, w is the width, and t is the thickness of the AFM probe, and H is the length of the AFM tip. E, and G are also the young's modulus, and shear modulus of the AFM respectively.

Since the width of the AFM probe (w) is much greater than its thickness (t) (w>>t), normal deflection and lateral twisting are more compliant than lateral deflection. Spring forces and moments are a linear product of the spring constants (K_y, K_z, K_Θ) and deflections y_p, z_p, Θ (eqs. 4-6).

$$F_y = K_y y_P \tag{4}$$

$$F_z = K_z z_P \tag{5}$$

$$M_\theta = K_\theta \theta \tag{6}$$

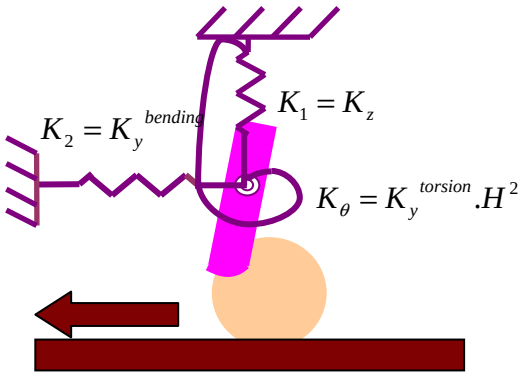

Figure 3. Lumped modeling and stiffness coefficients of the AFM probe cantilever.

Mass-spring lumped modeling of the AFM is a valid assumption for small deflections and reveals a realistic motion of the probe. Damping factors are negligible as the substrate is moved with slow velocity.

Spring forces and moment (F_y, F_z, M_Θ), shear force (V), normal and lateral tip forces (F_Z, F_Y), and tip pushing force (F_T) are depicted during lateral movement of the nano-particle in an AFM tip free-body diagram, below (figure 4). Forces are proportional to the angle of twist Θ (z_P and Θ are dependent), and also the y_P deflection of the AFM probe.

$$y_P = y_{sub.} + (R_P - \delta_t)\sin\varphi - H\sin\theta$$

$$z_P = z_{sub.} + (R_P - \delta_t)\cos\varphi + (R_P - \delta_s) + H\cos\theta \tag{7}$$

Elastic deformation (δ) rates are assumed to be negligible.

$$\ddot{y}_P = \ddot{y}_{sub.} - \ddot{\delta}_t \sin\varphi - H\ddot{\theta}\cos\theta + H\dot{\theta}^2 \sin\theta$$

$$\ddot{z}_P = \ddot{z}_{sub.} - \ddot{\delta}_t \cos\varphi - \ddot{\delta}_s - H\ddot{\theta}\sin\theta - H\dot{\theta}^2\cos\theta \quad (8)$$

Equations of motion (EOM) for the AFM in normal (z) and lateral (y) directions, plus lateral twisting follow:

$$\sum \vec{F}_y = m\vec{a}_y$$

$$F_Y - F_y - V\cos\theta = m\ddot{y}_{\otimes} = m\left(\frac{\ddot{y}_T + \ddot{y}_P}{2}\right) \quad (9)$$

$$\sum \vec{F}_z = m\vec{a}_z$$

$$F_Z - V\sin\theta - F_z = m\ddot{z}_{\otimes} = m\left(\frac{\ddot{z}_T + \ddot{z}_P}{2}\right) \quad (10)$$

$$\sum \vec{M}_{(P)}^{+} = I_P\ddot{\theta}$$

$$-M_\theta + F_Z H\sin\theta + F_Y H\cos\theta = I_P\ddot{\theta} \quad (11)$$

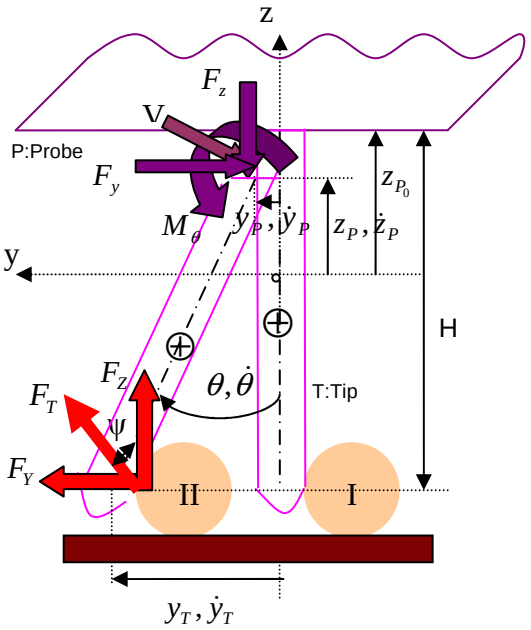

Figure 4. Free-body-diagram of the AFM tip and corresponding angular and linear displacements.

Substituting spring forces in EOM, tip forces are calculated in terms of position variables Θ, y_P.

$$F_Z = \left(\frac{I_P\ddot{\theta} + M_\theta}{H}\right)\sin\theta + F_z\cos^2\theta - F_y\sin\theta\cos\theta$$
$$- m\cos\theta\left(\frac{H}{2}\dot{\theta}^2 + \ddot{\delta}_t\cos(\theta+\varphi) + \ddot{\delta}_s\cos\theta\right) \quad (12)$$

$$V = \frac{1}{\sin\theta}\left[F_Z - F_z + m\left(\frac{H}{2}\ddot{\theta}\sin\theta + \frac{H}{2}\dot{\theta}^2\cos\theta + \ddot{\delta}_t\cos\varphi + \ddot{\delta}_s\right)\right] \quad (13)$$

$$F_Y = F_y + V\cos\theta + m\left[\frac{H}{2}\left(-\ddot{\theta}\cos\theta + \dot{\theta}^2\sin\theta\right) - \ddot{\delta}_t\sin\varphi\right] \quad (14)$$

$$F_T = \sqrt{F_Y^{\,2} + F_Z^{\,2}} \quad , \quad \psi = \tan^{-1}\left(F_Y / F_Z\right) \quad (15)$$

The above equations are a nonlinear set of 2nd order ordinary differential equations (ODE's). It is impossible to analytically solve this problem. The problem is numerically solved using the Runge-Kutta method (ODE45 in Matlab).

To simplify the problem, assume Θ, y_P, and their derivatives as four independent state variables. This is defined in equations 16 to 19.

$$y_1 = \theta \quad (16)$$

$$y_2 = \dot{\theta} = \frac{dy_1}{dt} \quad (17)$$

$$y_3 = y_P \quad (18)$$

$$y_4 = \dot{y}_P = \frac{dy_3}{dt} \quad (19)$$

Four state-space algebraic equations of 21 to 24 in the form of equation 20 are defined.

$$\frac{dy_i}{dt} = f(y_1, y_2, y_3, y_4);\ i = 1..4 \quad (20)$$

$$\frac{dy_1}{dt} = \dot{\theta} = y_2 \quad (21)$$

$$\frac{dy_2}{dt} = \ddot{\theta} = \frac{1}{I_P}\left(-K_\theta y_1 + F_Z H\sin y_1 + F_Y H\cos y_1\right) \quad (22)$$

$$\frac{dy_3}{dt} = \dot{y}_P = y_4 \quad (23)$$

$$\frac{dy_4}{dt} = \ddot{y}_P = \frac{1}{m}\left(F_Y - K_y y_3 - V\cos y_1\right)$$
$$-\frac{H}{2}\left(\frac{dy_2}{dt}\cos y_1 - y_2^{\,2}\sin y_1\right) \quad (24)$$

Initial conditions (I.C.'s) in equation 25 are applied to solve for dynamics of the AFM at every moment.

$$\begin{cases} z_{P_0} = L\sin(\phi_0),\ \phi_0 = 0.7^\circ \\ \dot{z}_{P_0} = \dot{z}_{T_0} \\ \ddot{z}_{P_0} = -\dfrac{\dot{y}_{sub.}^{\,2}}{H} \end{cases} \quad \begin{cases} z_{T_0} = -(H - z_{P_0}) \\ \dot{z}_T = -\dot{\delta}_t\cos\varphi - \dot{\delta}_s = const \\ \ddot{z}_T = 0 \end{cases}$$

$$\begin{cases} y_{P_0} = 0 \quad , P: Probe \\ \dot{y}_P = \dot{y}_T - H\dot{\theta}\cos\theta \\ \ddot{y}_{P_0} = 0 \end{cases} \quad \begin{cases} y_{T_0} = 0 \quad , T: Tip \\ \dot{y}_T = \dot{y}_{sub.} - \dot{\delta}_t\sin\varphi = const. \\ \ddot{y}_T = 0 \end{cases}$$

$$\begin{cases} \theta_0 = 0 \\ \dot{\theta}_0 = \dfrac{\dot{y}_{sub.}}{H} \\ \ddot{\theta} = 0 \end{cases} \quad \begin{cases} \delta_{t/s} \quad t: tip\ , \quad s: sub. \\ \dot{\delta}_{t/s} = const. \\ \ddot{\delta}_{t/s} = 0 \end{cases} \quad (25)$$

In the sticking phase, nanoparticles stick to the substrate and they move with the same velocity $\dot{y}_{sub.}$. However the friction force increases to its critical value when the slipping phase starts (figure 6). In the slipping phase, the dynamics of the AFM are independent of the substrate.

In the sticking phase, f_s increases to its critical value. The dynamic coefficient of friction μ_d remains constant during the

slipping phase. Friction coefficients between the tip-particle and the particle-substrate vary, according to figure 6.

In figure 5, the diagram of the sticking and slipping phases is summarized. In the sticking phase the particle kinematics y, z are known and the problem is solved to find the AFM dynamics and forces F_T. When the AFM pushing force satisfies the slipping force condition F^*, slipping loop begins. In the slipping phase, the AFM dynamics F_T is known and the problem is solved to find the nanoparticle kinematics and position $y_{par.}$. The loop ends when the desired position of the nanoparticle is achieved.

In part B, nanoparticle modeling is discussed.

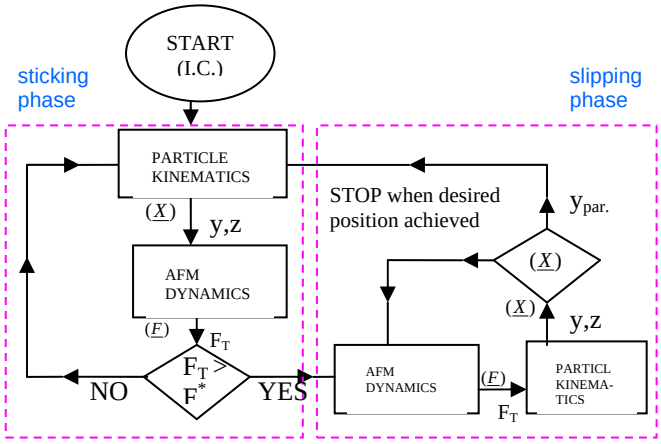

Figure 5. Phase algorithm shows how to derive unknown parameters at every moment.

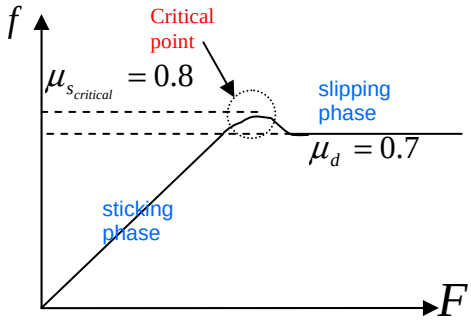

Figure 6. Static and dynamic friction coefficients

B. Nanoparticle Model

Nanoparticle dynamics and forces are considered and shown in figure 7, when the particle is pushed by AFM tip. Particle-Substrate friction force f_s can be written in terms of AFM pushing force magnitude F_T and angle ψ:

$$f_s = F_Y = F_T \sin\psi \tag{26}$$

In order for a nanoparticle to start sliding on the substrate, the following criteria should be satisfied [8], [14], [18]:

$$f_s > \mu_s F_s + \tau_s A_s \tag{27}$$

where nanoparticle friction coefficient μ_s, and shear strength τ_s on substrate, are assumed to be constant, and equal to the ones on tip, respectively. The normal force and contact area are defined as both the pushing and the adhesion forces:

$$F_s = F_Z = F_T \cos\psi \tag{28}$$

$$A_s = \pi(a_s{}^3)^{2/3} \tag{29}$$

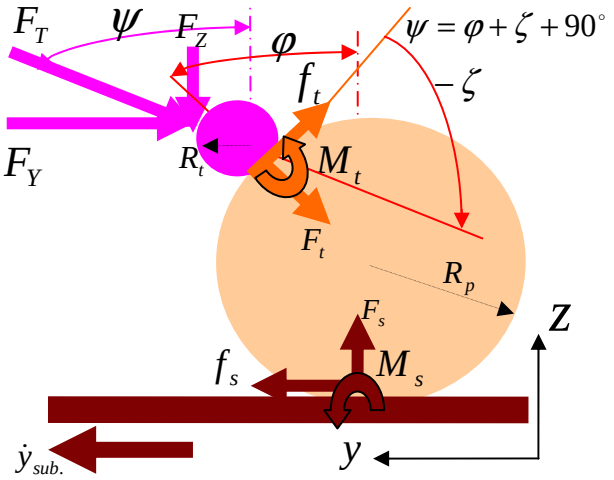

Figure 7. Particle dynamics and forces during nanoparticle manipulation.

Forces required to separate two surfaces are mainly proportional to the equivalent radius and adhesion energy between contacting surfaces. Using the Johnson-Kendall-Roberts (JKR) model ([2], [13], [15]), contact radius (a) and indentation depth (δ) are derived as:

$$a^3 = \frac{R'}{K}\left[F + 3\pi R'\omega + \sqrt{6\pi R'\omega F + (3\pi R'\omega)^2}\right] \tag{30}$$

$$\delta = \frac{a^2}{R'} - \frac{2}{3}\sqrt{3\pi\omega a / K} \tag{31}$$

where $\omega=2\gamma$, and γ are the particle and tip/substrate interfacial adhesion and surface energy respectively. Assume $R=R_p$, $F=F_s$ for particle deformation on substrate, and $R=R_pR_t/(R_p+R_t)$, $F=F_t$ for particle deformation on tip, where R_p is the particle radius, R_t is the tip radius, and K is the equivalent modulus of elasticity of the materials in contact.

In nanoscale, these deformations are in the order of particle size and should be considered; these are less important in macro-scale because adhesion forces are of smaller magnitude than pushing forces [12].

SIMULATION AND DISCUSSION

In this simulation, a R_p=50 nm gold particle is moved on the silicon oxide substrate. The AFM tip radius is R_t=20 nm. Surface energy between the nanoparticle and the tip/substrate is ω=0.2 J/m^2. The constant friction coefficients for static and dynamic motion of the nanoparticle on the substrate are μ_s=0.8, and μ_d=0.7, respectively. Shear strength is assumed to be τ_s=28 N/m^2, and constant on the both contact surfaces between the particle and the tip/substrate. The AFM tip is composed of single crystal silicon. The geometric constants and mechanical properties of the AFM are summarized in tables 1 and 2.

H (μm)	L (μm)	S=H/L	w (μm)	t (μm)
12	225	0.0533	48	1

Table 1. The AFM geometric constants.

E (GPa)	ν	G (GPa)	ρ (kg/m^3)
169	0.27	66.54	2330

Table.2. The AFM mechanical properties.

The AFM contacts with a target nanoparticle for the purpose of manipulation. To locate a target particle, the substrate and then the target nanoparticle should first be scanned and recognized. During scanning, the AFM runs in the tapping mode to avoid undesirable movements of the particle. For manipulation, the AFM mode is changed to the contact mode.

Step procedures for controlled pushing of a particle can be summarized as follows [11]:

1. An image is recorded in the vibrating cantilever intermittent contact mode.
2. The tip is positioned behind the particle.
3. The probe vibration is turned off.
4. The particle is pushed to a selected location.
5. The AFM is switched back into the vibrating cantilever mode, and the pushed particle image is held by scanning in the intermittent contact mode.

To reduce the spinning factor, which leads to separation of the AFM tip and particle, central contact with no x-axis offset (x_0=0) is required. In the pushing zone (φ>0), bigger contact angles decrease the critical sliding force on the substrate and are therefore encouraged. After the AFM approach and contact with the particle, any slipping between tip and particle should be restricted. This can be achieved only if the design parameters restrict any slipping on the tip, and slipping on substrate is more dominant. When the set up is ready for manipulation, the stage starts to move laterally in y-axis, with a constant velocity. Therefore, the substrate, particle, and the AFM move together, while the substrate and the particle are stuck together. During the sticking phase, the lateral force (F_Y) on the AFM tip increases due to lateral deflection and twisting of the probe. Changes in normal force (F_Z) due to probe twisting, are very small since the tip-particle contact point does not change. Therefore the pushing force magnitude (F_T), and angle (ψ) increases over time depending on the increase in the lateral force.

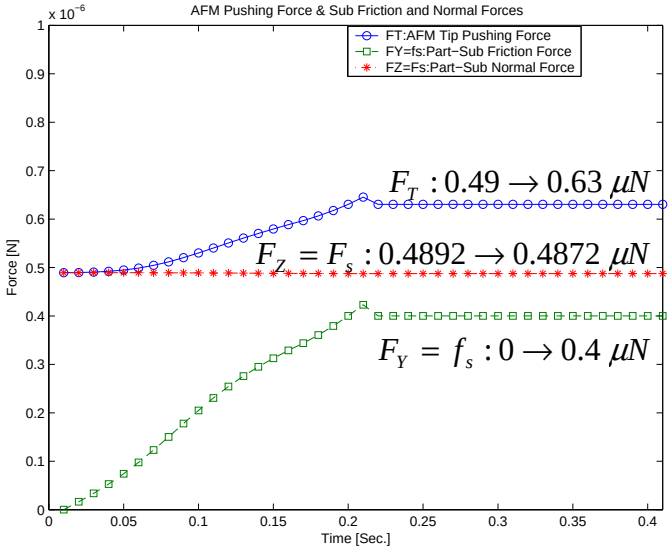

Figure 8. Force variations in AFM and nanoparticle; normal, lateral, and pushing force.

On the other hand, the changes in the AFM configuration and pushing force could be traced and compared with the critical friction forces at the contact points. According to the mode diagrams, it can be determined when slipping/rolling starts; based on that, the pushing procedure can be designed. For example, if the particle starts to slip on the substrate after 0.2 seconds (which means the pushing force has reached the critical slipping force on the substrate), the AFM tip will prevent the nanoparticle from moving with the substrate (figure 9).

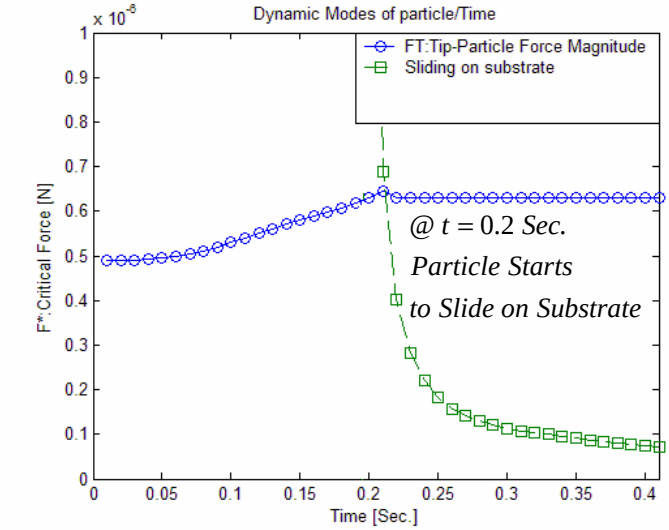

Figure 9. AFM pushing force meets nanoparticle critical sliding force and then stays constant during dynamic motion of the nanoparticle.

Based on the slipping period, a new position of the nanoparticle can be calculated, which can be used as a basic tool for accurate manipulation.

Assume that the substrate velocity is 100 nm/s; after 0.2 seconds, the 50 nm particle begins to slip on the substrate. To move the nanoparticle 21 nm in the y-axis negative direction, the simulation should run for 0.4 seconds.

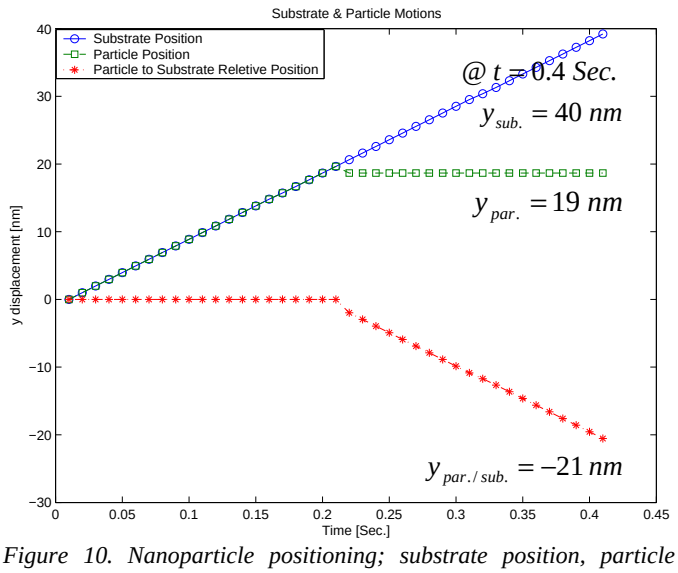

Figure 10. Nanoparticle positioning; substrate position, particle position, and particle to substrate position after 0.4 Sec.

Based on the substrate velocity and the friction characteristics of the materials, the manipulation procedure can be designed. The following graph shows how the change in friction coefficient will affect the starting slip point on the substrate.

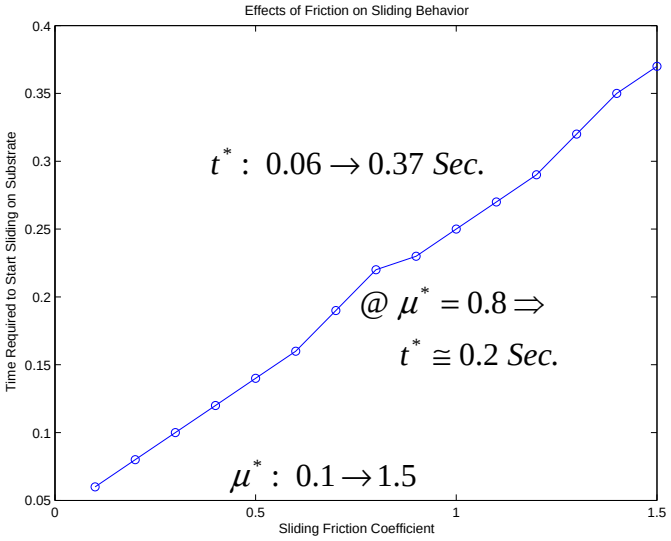

Figure 11. Effects of friction coefficient on the sliding behavior.

Other parameters such as surface adhesion, particle diameter, contact force and angles, are important factors in a precise manipulation scheme. The following mode diagram demonstrates the critical sliding force required to overcome sticking [31].

To check the new location of the nano-particle, a non-contact mode AFM is used to scan the position of the particle.

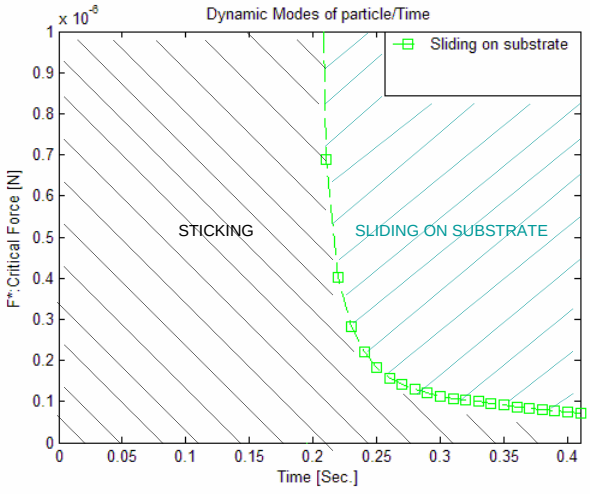

Figure 12. Mode diagram depicts required critical force to overcome sticking when the particle is pushed by the AFM.

The assumption of a rigid particle is no more valid when soft materials with high pseudo-elastic properties are examined. To consider elastic deformation at the points of contact, the JKR model is used. When two spheres, or one sphere with a flat surface come into contact, elastic deformation causes a circular shape interface at the contact region. Due to this deformation, the center of the contacting spheres comes closer, according to the indentation depths.

In nanoscale, this change is in the order of sphere radius and can not be disregarded. In this paper, all the deformations are calculated.

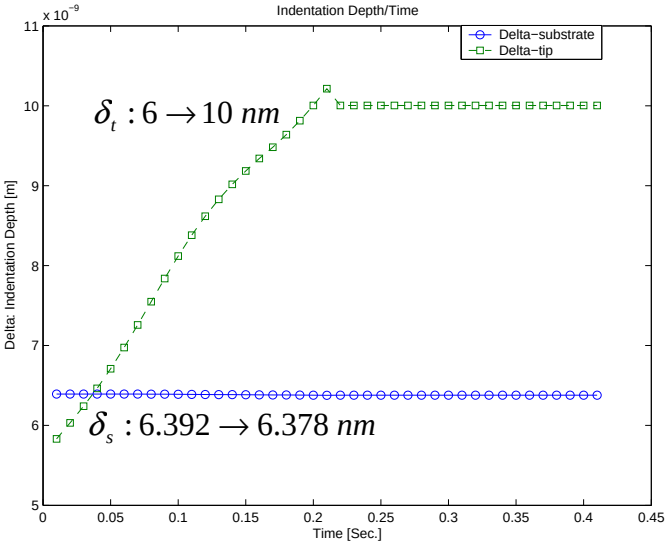

Figure 13. Indentation depth of the particle on the tip/substrate alters during pushing phase.

In figure 13, it is shown that as pushing force increases, the contact area and the indentation depth between the tip and the particle both increase. At the same time, the contact area and the indentation depth between particle and substrate are both decreasing. Since it is anticipated that slipping and separation on the substrate occur first, while the AFM maintains its pushing contact, this is in good agreement with simulation results.

Rolling behavior should be considered when the size of the particle is more than 1 µm [3], [9], [30]. In smaller particles, sliding behavior is more dominant. According to the results of the numerical solution, nanoparticle pushing simulation is developed (figure 14). The nanoparticle motion can be visually traced in a real time. The advantage of this simulation is that the dynamic behavior of the nanoparticle is observed before setting up the real experiment. It also provides a better understanding of the nanoscale world.

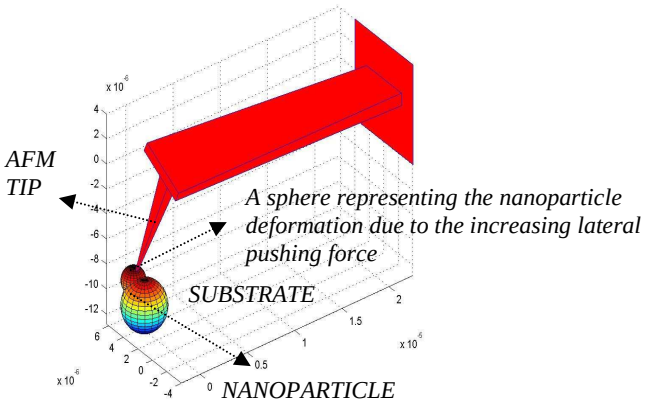

Figure 14. Nano-particle pushing simulation when substrate is moving with a constant velocity

CONCLUSION

In this paper, nanoparticle positioning, using the AFM as a nanoprobe manipulator, is modeled and dynamic behavior of the particle is defined. After scanning the substrate to achieve a detailed map of the particles on the substrate, the AFM tip is brought into contact with the particles as a manipulation tool. Then the substrate begins to move laterally, which helps the lateral force on the AFM tip to increase and reach the critical force required for particle movement. Depending on the parameters of the simulation and the tribological characteristics of the materials, various behaviors of the particle can be predicted. If the simulation continues to run for a known period, a new map of the particle can be drawn which locates the new particle position. By controlling the substrate velocity and mapping the location of particles at every moment, positioning of nano-particles can be achieved. Designing simulation values not only achieves the desired dynamics to better understand real-time simulation, they are also very effective tools for establishing valid experiments.

Based on the simulation results, sliding occurs first and is more likely to occur for smaller particles rather than rolling. However, sliding and rolling can be observed simultaneously if the applied force increases above both critical limits. In a pushing zone, particle sliding on the substrate occurs earlier than sliding on the tip. Less force is required in order to manipulate smaller particles but to overcome the critical forces, a minimum manipulation force is required.

The future work is to use these methods as basic tools for nanoparticle manipulation control. These models will be validated experimentally. Additionally, a feedback control system is being developed to automatically position and characterize nanoparticles.

ACKNOWLEDGMENTS

We are grateful to our NanoRobotics Laboratory members for their valuable suggestions during this research.

REFERENCES

[1] Ashhab, M., Salapaka, M. V., Dahleh, M., and Mezic, I., "Dynamic Analysis and Control of Microcantilevers", Automatica, Vol. 35, No. 10, pp. 1663-1670, 1999.

[2] Bhushan, B., Introduction to Tribology, John Wiley & Sons, New York, 2002.

[3] Brilliantov, N. V., and Poschel T., "Rolling as a Continuing Collision", *The European Physical Journal B*, Vol. **12**, pp. 299-301, 1999.

[4] Butt H., "A Technique for Measuring the Force Between a Colloidal Particle in Water and a Bubble", *J. Colloidal and Interface Science*, Vol. **166**, pp. 109-117, 1994.

[5] Carpick, R. W., Agrait, N., Ogletree, D. F., and Salmeron, M., "Variation of the Interfacial Shear Strength and Adhesion of a Nanometer-Sized Contact", *Langmuir*, Vol. **12**, pp. 3334-3340, 1996.

[6] Chen, J., Workman, R. K., Sarid, D., and Hooper, R., "Numerical Simulation of a Scanning Force Microscope with a Large-Amplitude Vibrating Cantilever", *Nanotechnology*, Vol. **5**, pp. 199-204, 1994.

[7] Dedkov, G., "Friction on the Nanoscale: New Physical Mechanism", *Meterials Letters*, Vol. **38**, pp. 360-366, 1999.

[8] Falvo, M. R., and Superfine, R., "Mechanics and Friction at the Nanometer Scale", *J. Nanoparticle*, Res. **2**, pp. 237-248, 2000.

[9] Falvo, M. R., Taylor, R. M., Helser, A., Chi, V., Brooks Jr, F. P., Washburn, S., and Superfine, R., "Nanometre-Scale Rolling and Sliding of Carbon Nanotubes", *Nature*, Vol. **397**, pp. 236-238, 1999.

[10] Fearing, R.S., "Survey of Sticking Effects for Micro Parts Handling", *Proc. of IEEE MEMS*, pp. 212-217, 1995.

[11] Hansen, L. T., Kuhle, A., Sorensen, A. H., Bohr, J., and Lindelof, P. E., "A Technique for Positioning Nanoparticles Using an Atomic Force Microscope", *Nanotechnology*, Vol. **9**, pp. 337-342, 1998.

[12] Heim, L., Blum, J., Preuss, M., and Butt, H., "Adhesion and Friction Forces between Spherical Micrometer-Sized Particles", *Physical Review Letters*, Vol. **83**, No. 16, pp. 3328-3331, 1999.

[13] Israelachvili, J., Intermolecular and Surface Forces, Academic Press London, 2nd Edition, 1992.

[14] Johnson, K. L., "The Contribution of micro/nano-tribology to the interpretation of dry friction", *Proc. of IMechE*, Vol. **214**, Part C, 2000.

[15] Johnson, K. L., Contact Mechanics, Cambridge University, London, 1985.

[16] Junno, T., Deppert, K., Montelius, L., and Samuelson, L., "Controlled Manipulation of Nanoparticles with an Atomic Force Microscope", *Appl. Physics Letters*, Vol. **66**, pp. 3627-3629, June 1995.

[17] Laxminarayana, K., and Jalili, N., "A Review of Recent Developments in Atomic Force Microscopy Systems with Application to Manufacturing and Biological Processes", *Proc. of IMECE*, Washington, USA, November 2003.

[18] Meyer, E., Overney, R. M., Dransfeld K., and Gyalog, T., "Nanoscience: Friction and Rheology on the Nanometer Scale", *World Scientific Pub.*, Singapore, 1998.

[19] Miyazaki, H., and Sato, T., "Mechanical Assembly of Three-Dimensional Microstructures from Fine Particles", *Advanced Robotics*, Vol. **11**, No. 2, pp. 169-185, 1997.

[20] Ramachandran, T. R., Baur, C., Bugacov, A., and et al., "Direct and Controlled Manipulation of Nanometer-Sized Particles Using the Nan-Contact Atomic Force Microscope", *Nanotechnology*, Vol. **9**, pp. 237-245, 1998.

[21] Saito, S., Miyazaki, H. T., Sato, T., Takahashi, K., "Kinematics of Mechanical and Adhesional Micromanipulation under a Scanning Electron Microscope", *Journal of Applied Physics*, Vol. **92**, No. 9, pp. 5140-5149, 2002.

[22] Saito, S., Miyazaki, H. T., and Sato, T., "Micro-object Pick and Place Operation under SEM based on Micro-Physics", *J. Robotics and Mechatronics*, Vol. **14**, No. 3, pp. 227-237, 2002.

[23] Salapaka, S., and Dahleh, M., "A Model for Friction in Atomic Force Microscopy", *Proc. of the American Control Conf.*, Chicago, USA, June 2000.

[24] Schafer, D., Reifenberger, R., Patil, A., and Andres, R., "Fabrication of Two-dimensional Arrays of Nanometer-Size Clusters with the Atomic Force Microscope", *Appl. Physics Letters*, Vol. **66**, pp. 1012-1014, 1995.

[25] Sitti, M., "Teleoperated and Automatic Manipulation Systems Using Atomic Force Microscope Probes", *Proc. of IMECE*, Washington, USA, November 2003.

[26] Sitti, M., "Atomic Force Microscope Probe Based Controlled Pushing for Nano-Tribological Characterization", *IEEE/ASME Transaction on Mechatronics*, Vol. **9**, No. 2, June 2004 (to appear).

[27] Sitti, M., and Hashimoto, H., "Teleoperated Touch Feedback from the Surfaces at the Nanoscale: Modeling and Experiments", *IEEE/ASME Transactions on Mechatronics*, Vol. **8**, No. 1, March 2003.

[28] Sitti, M., and Hashimoto, H., "Controlled Pushing of Nanoparticles: Modeling and Experiments", *IEEE/ASME Transactions on Mechatronics*, Vol. **5**, No. 2, June 2000.

[29] Sitti, M., and Hashimoto, H., "Two-Dimensional Fine Particle Positioning under Optical Microscope using a Piezoresistive Cantilever as a Manipulator", *Journal of Micromechatronics*, Vol. **1**, No. 1, pp. 25-48, 2000.
[30] Soltani, M., and Ahmadi, G., "Particle Removal Mechanisms under Substrate Acceleration", *Journal of Adhesion*, Vol. **44**, pp. 161-175, 1994.
[31] Tafazzoli, A., and Sitti, M., "Dynamic Modes of Nano-Particle Motion during Nanoprobe Based Manipulation", *Proc. of 4th IEEE Conf. in Nanotechnology*, Munich, Germany, August 2004 (to appear).
[32] Zesch, W., and Fearing, R. S., "Alignment of Microparts Using Force Controlled Pushing", *SPIE Conf. on Microrobotics and Micromanipulation*, Boston, USA, November 1998.